Stable hydrogen and oxygen isotopic compositions of water vapor in volcanic plumes sampled in glass bottles using cavity ring-down spectroscopy

Koji U. Takahashi [a,b,*], Urumu Tsunogai [a], Fumiko Nakagawa [a], Chiho Sukigara [a,1]

[a] Graduate School of Environmental Studies, Nagoya University, Nagoya, Japan
[b] Research Institute for Geo-Resources and Environment, Geological Survey of Japan, National Institute of Advanced Industrial Science and Technology, Tsukuba, Japan

ABSTRACT

The isotopic compositions (δ^2H and δ^{18}O) of fumarolic H_2O emitted during volcanic eruptions can distinguish the type of eruption (magmatic or phreatic), but direct sampling of fumarolic H_2O in eruptive volcanoes is often neither practical nor safe. In this study, we developed a new analytical system to safely determine the isotopic compositions of fumarolic H_2O from the volcanic plume samples taken in glass bottles. The system consisted of stainless steel gas introduction line and a cavity ring-down spectroscopic unit. In the 1 L glass sample bottles, analytical precision (1σ) was estimated to be better than 2‰ and 0.3‰, respectively, when >3400 ppmv of H_2O was introduced, and better than 3‰ (δ^2H) and 0.4‰ (δ^{18}O) when >1800 ppmv of H_2O was introduced. The H_2O concentration accuracy was better than 5%. Using this in-situ collection method and the analytical system, we determined the isotopic compositions of H_2O in volcanic plume samples taken at Iwo-yama in the Kirishima volcano group (Japan), and deduced the isotopic composition of fumarolic H_2O from the volcanic plume. The reciprocal of the H_2O concentration in the plume samples showed a good linear relationship with the isotopic composition. The isotopic composition of fumarolic H_2O from Iwo-yama estimated from the plume samples directly corresponded to the determined fumarolic H_2O. This method improves upon previous analyses to obtain the isotopic compositions of fumarolic H_2O, particularly by reducing tedious, time consuming, and dangerous sampling of water vapor at volcanic fumaroles.

1. Introduction

Water vapor (H_2O) is the major component in fumarolic gas emitted from active volcanoes, followed by carbon dioxide, sulfur compounds (H_2S and SO_2), and variety of minor and trace gas species (e.g., Giggenbach, 1987; Giggenbach and Matsuo, 1991; Shinohara, 2005; Ohba et al., 2011). Magmatic and meteoric H_2O are assumed to be the principal components of H_2O in fumarolic gas (here after called fumarolic H_2O). The use of H and O isotope ratios can distinguish the origin of fumarolic H_2O (Craig, 1963; Matsuo et al., 1974, 1985). For instance, we would expect δ^2H values of -24.5 ± 7.3‰ and δ^{18}O values of $+6.0 \pm 3.0$‰ (average and 1σ of H_2O samples taken from high temperature fumaroles) for magmatic H_2O from convergent plate volcanoes (Giggenbach, 1992). We would also expect that, for meteoric H_2O

(i.e., groundwater), the isotopic compositions would plot on the local meteoric line of each volcano (Craig, 1963; Giggenbach, 1992).

Volcanic eruptions are mainly classified as either magmatic or phreatic (Barberi et al., 1992). Both types of eruptions will emit water with a mix of magmatic and meteoric water. Most phreatic eruptions are caused by heating meteoric H_2O with magma, so that most volcanic H_2O emitted during phreatic eruptions will consist of meteoric H_2O. In contrast, volcanic H_2O emitted during magmatic eruptions will be rich in magmatic H_2O compared with phreatic eruptions. Thus, the δ^2H and δ^{18}O of fumarolic H_2O emitted during eruptions may be able to differentiate the type of volcanic eruptions (magmatic or phreatic), and can also be used to detect temporal changes in a volcanic/hydrothermal system from changes in the H_2O isotopic compositions.

Direct sampling of fumarolic H_2O in eruptive volcanoes, however, is often neither practical nor safe. Instead, volcanic plumes are more safely sampled at a distance from a volcanic crater (Shinohara et al., 2008; Aiuppa et al., 2010,2011; Tsunogai et al., 2011, 2016). Since volcanic plumes are formed from mixing between fumarolic gas and atmospheric air, the fumarolic H_2O isotopic compositions can be estimated from the concentration and isotopic composition of volcanic plume

* Corresponding author at: Central 7, 1-1-1, Higashi, Tsukuba 305-8567, Ibaraki, Japan.
  E-mail address: koji-takahashi@aist.go.jp (K.U. Takahashi).
[1] Present address: Center for Marine Research & Operations, Tokyo University of Marine Science and Technology, Tokyo, Japan.

H_2O, by subtracting contribution from atmospheric H_2O (Tsunogai et al., 2011, 2016).

Traditionally, the isotopic compositions of atmospheric H_2O has been determined through collecting water vapor in cold traps, and then measuring the isotopic compositions for the collected H_2O (liquid) using isotope ratio mass spectrometers (IRMS) (e.g., Craig, 1961; Craig and Gordon, 1965; Uemura et al., 2008; Ueta et al., 2014; Yu et al., 2015). Although this method, called the cold trap method, is still widely used to obtain accurate isotopic compositions of water vapor in air and fumarolic gas, it is difficult to use for the determination of H_2O isotopic compositions in volcanic plumes. A sampling time of >10 min is needed to collect sufficient H_2O to measure isotopes with the traditional cold trap method (e.g., Wen et al., 2008; Iannone et al., 2010; Ueta et al., 2013), but instantaneous sampling is needed to obtain concentrated volcanic plume material ejected from eruptive volcanoes using aircraft (Tsunogai et al., 2016). Furthermore, traditional methods require a continuous supply of refrigerants such as ice, dry ice, or liquid nitrogen during sampling, and it is often difficult to bring these into a volcanic plume. As a result, we developed an alternative method, which enables us to obtain each sample instantaneously and without using refrigerants.

Based on slight differences in atomic adsorption spectrum between each isotopologue of H_2O, laser spectroscopic techniques have been developed to determine the isotopic compositions of H_2O (Kerstel, 2004). These techniques have been successfully applied to in-situ stable isotopic analysis of atmospheric water vapor in recent years (Lee et al., 2005; Griffith et al., 2006; Gupta et al., 2009; Schneider and Hase, 2009; Iannone et al., 2010; Tremoy et al., 2011; Bastrikov et al., 2014). However, they require electrical power (~150 W) for the measurements (Picarro, Inc, 2012) and the total weight of the devices and equipment (e.g., spectroscopic analyzer, computer, pump, and battery) exceeds 20 kg. As a result, it is not practical to bring them into areas with volcanic plumes (mountainous regions in most cases), which therefore precludes in-situ determination of volcanic plume H_2O isotopic compositions. Instead, it is more practical to collect volcanic plume samples in glass bottles and then bring them back to the laboratory for analysis, as already being done for H_2 in volcanic plume (Tsunogai et al., 2011, 2016). The carbon isotopic composition of fumarolic CO_2 has also been estimated from the concentration and isotopic composition of volcanic plume CO_2, by subtracting contribution from atmospheric CO_2 (Rizzo et al., 2014, 2015; Fischer and Lopez, 2016; Malowany et al., 2017).

In this study, we developed an original system to introduce gas samples collected in glass bottles into a cavity ring-down spectroscopy (CRDS) to analyze the δ^2H and $\delta^{18}O$ of H_2O in volcanic plume samples. Here we report details of the analytical system and evaluated its performance. Using this system, we also determined the concentration and the isotopic compositions of H_2O in volcanic plume samples, and used our in-situ collection method to estimate the isotopic compositions of fumarolic H_2O.

2. Experimental

2.1. Analytical procedure

2.1.1. Air/volcanic plume samples (bottle samples)

We used 1 L glass bottles with two stopcocks sealed by Viton o-rings at both ends to take the volcanic plume samples; the samples were also stored in these bottles until analysis. All of the glass bottles were evacuated to $<10^{-4}$ Pa under 60 °C in the laboratory to remove residual water vapor. Then, each bottle was filled with an air/volcanic plume sample to the surrounding atmospheric pressure in the study area (Tsunogai et al., 2003, 2011) and stored for <2 weeks until isotope analysis in the laboratory. The sampling time needed for each bottle sample was 20 s. Before the isotopic analysis, the internal pressure of 1 L glass bottles were measured by the vacuum line equipped with a pressure gauge.

To analyze the concentration and isotopic compositions (δ^2H and $\delta^{18}O$) of H_2O in a sampled volcanic plume, a stainless steel gas inlet system was developed and connected with a CRDS water isotope analyzer L2120-i instrument (Picarro Inc., Santa Clara, CA, USA) via an automated 2-position, 3-port switching valve (Valve 1), which introduced the bottled air sample (Fig. 1). The instrument was also equipped with a A0211 vaporizer and auto-sampler (PAL HTS-xt) to determine the isotopic compositions of liquid H_2O (Fig. 1). We used Valve 1 to switch the type of sample to be analyzed from liquid H_2O to water vapor in air/volcanic plume samples. The gas introduction line was equipped with 2 valves controlled manually: a 2-position, 6-port switching valve (Valve 2) and a needle stop valve (Valve 3).

Prior to analysis, the sample bottle was connected to the injection port of the gas inlet system and warmed to 60 °C for 15 min using a cylindrical heater. Then, the entire system, including the CRDS, was purged with high-purity air (N_2: 79% and O_2: 21%), until the H_2O concentration was <100 ppmv. This was done by setting the three valves of the gas introduction line to their ordinal positions: (1) Valve 1 was in the 'Water vapor mode' position; (2) Valve 2 was placed in the 'Measure' position; (3) Valve 3 was set at the 'open' position (Fig. 1). Valve 3 was then closed to stop flushing the system with dry air, and the stopcock of a sample bottle was opened to introduce a portion of each air/volcanic plume sample into the CRDS for 480 s using the inner pressure gradient created by a diaphragm pump. The concentrations and isotopic compositions of H_2O in the volcanic plume/air samples were monitored for 480 s (120 data points) in the CRDS. The concentration and isotopic compositions of H_2O in each sample were calculated by averaging the data collected between 150 and 420 s. Then, the sample bottle stopcock was closed, and Valve 2 was set at the 'bypass' position to remove the sample bottle. After changing a sample bottle, Valve 2 was once again switched to the 'Measure' position, and Valve 3 was set to 'open' to allow line purging for the next measurement. Overall, it took about 20 min to flush the gas sample introduction line and get the CRDS analyzer to <100 ppmv H_2O. Thus, the total time needed for a single analysis was about 30 min.

2.1.2. Liquid samples

Liquid samples such as the standard waters (STDs) and water condensate from laboratory air and fumarolic gas were prepared by pipetting them into vials (2 mL glass short-thread vials, PTFE/silicone capped), after which the vaporizing cell was flushed with dry air by opening Valves A and B. Then, an aliquot (1.8 μL) of liquid sample was injected through a septum-sealed injection port into the vaporizer cell using the auto sampler and a 10 μL syringe (Schauer et al., 2016). The injected water samples were flash-evaporated at 110 °C in the cell and sent into the cavity as vapor by switching Valve 1 to the 'liquid mode' position and closing Valve B. The ordinal position of Valve 1 was 'water vapor mode' that purged the cavity and the line in the CRDS system with carrier gas (dry air) until measurements. All of the liquid water samples were measured in a high precision mode, which takes about 8 min per an injected sample (Gupta et al., 2009). We injected and measured the same water sample 8–10 times to achieve sufficient accuracy and precision. To minimize cross-contamination, the last three data points were used to calculate the isotopic compositions of the liquid H_2O sample. The analytical precision (1σ) of δ^2H and $\delta^{18}O$ values for liquid H_2O were 1‰ and 0.1‰, respectively.

2.2. Isotopic calibration

The hydrogen and oxygen isotope ratios are reported in delta (δ) notation ($\delta = R_{sample} / R_{std} - 1$). R_{sample} and R_{std} denote the isotope ratios ($^2H/^1H$ and $^{18}O/^{16}O$) of a sample and a standard (Vienna Standard Mean Ocean Water, VSMOW), respectively. We routinely calibrated the isotopic compositions of H_2O in the air/volcanic plume samples by using four liquid H_2O working standards STD1, STD2, STD3, and STD4, that exhibited +1.2‰, −73.5‰, −139.5‰, and −370.9‰ for δ^2H, respectively,
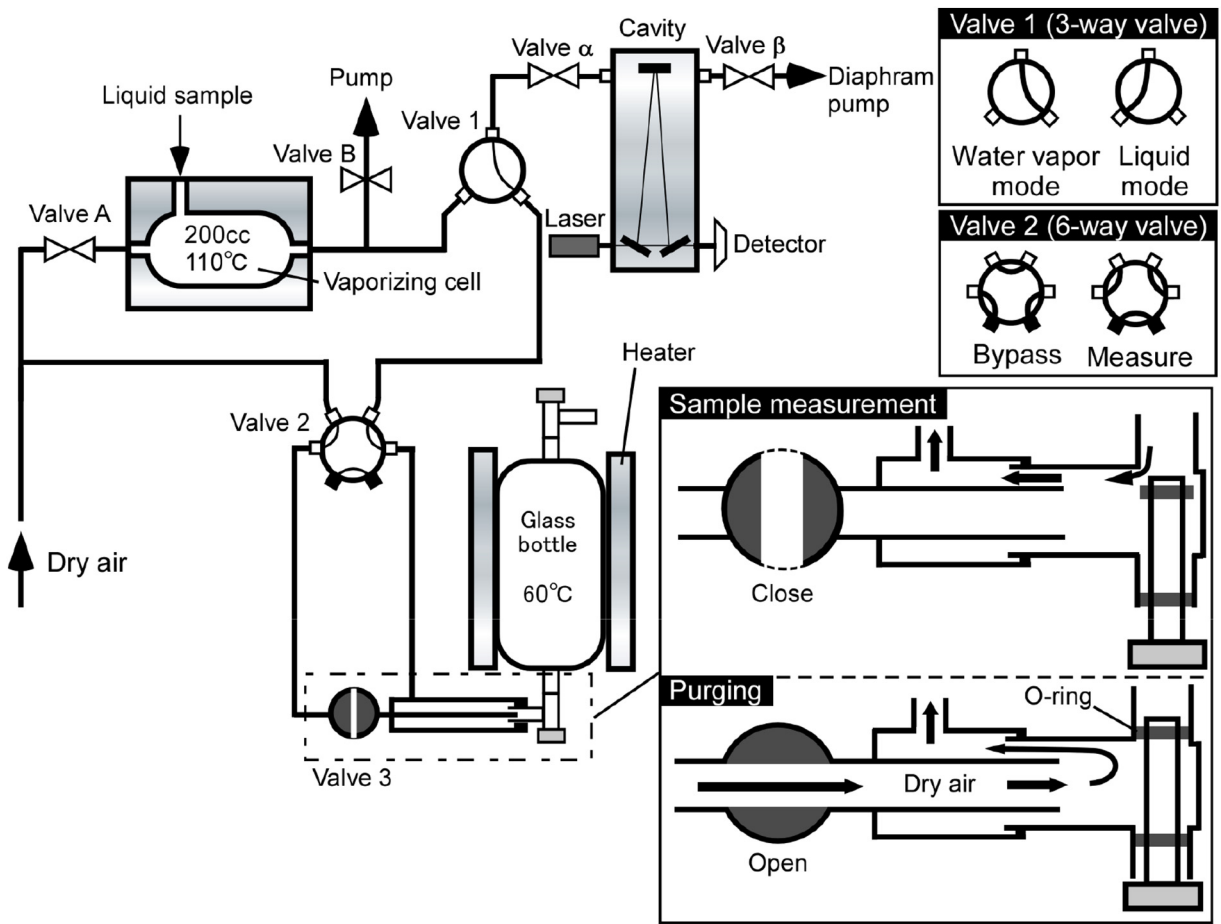
Fig. 1. Schematic of the analytical system used to determine concentrations and isotopic compositions of H_2O (water vapor) in air/volcanic plume samples taken in a glass bottle, together with the vaporizer (A0211) for liquid H_2O samples.

and −0.14‰ (STD1), −11.33‰ (STD2), −18.02‰ (STD3), and −46.61‰ (STD4) for $\delta^{18}O$. The δ^2H and $\delta^{18}O$ values of these working standards were precisely calibrated using the international standards (VSMOW and Standard Light Antarctic Precipitation, SLAP) (Coplen and Hopple, 1995). To estimate the isotopic compositions of H_2O in air/volcanic plume samples on the VSMOW scale, we measured the isotopic compositions (δ_{r_std}) daily of two of the four liquid standards using the new analytical system, by changing the water volume introduced to the vaporizing cell and adjusting the H_2O concentration at the CRDS to around 20,000, 7000, and 3000 ppmv, respectively. Then, we obtained the isotopic compositions (δ'_{r_std}) of each working standard in which the blank H_2O contribution had been corrected from the intercept of the linear relationship between $1/[H_2O]$ and δ_{r_std}.

We also estimated the concentration and isotopic compositions of blank H_2O as the intersection of the linear relationship between $1/[H_2O]$ and isotopic compositions for each working standard (Gelwicks and Hayes, 1990; Tsunogai et al., 2000), as shown in Fig. 2. The isotopic compositions of water vapor in each glass bottle were also measured and corrected for the contribution from blank H_2O using Eq. (1):

$$\delta'_{r\_spl} = (A_{r\_spl} * \delta_{r\_spl} - A_b * \delta_b)/(A_{r-spl} - A_b) \tag{1}$$

where δ'_{r_spl} denotes the corrected isotopic compositions of each water vapor sample, δ_{r_spl} and δ_b denote the isotopic compositions of sample H_2O (measured) and blank H_2O, respectively, and A_{r_spl} and A_b denote the concentration of sample H_2O (measured) and blank H_2O, respectively. After blank correction using Eq. (1) (see discussion in Section 3.1.), we calculated the isotopic compositions of each sample
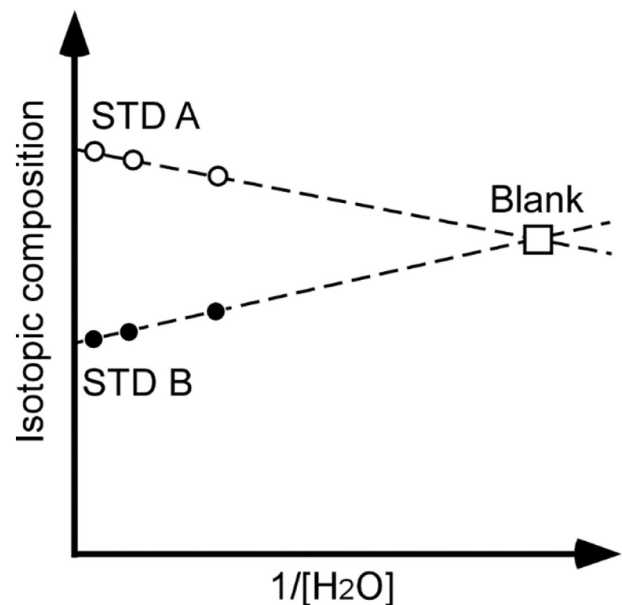

Fig. 2. The conceptual diagram showing blank estimation. Open and closed circles show changes in the measured isotopic compositions of two STDs in accordance with the reciprocal H_2O concentration ($1/[H_2O]$), respectively. The concentration and isotopic composition of blank H_2O (open square) as the intersection of the linear relationship between $1/[H_2O]$ and isotopic compositions for each working standard.

on the VSMOW scale, assuming a linear relationship between the measured and true isotopic compositions.

3. Results and discussion

3.1. Analytical blanks

We found that blank H_2O eluted from the system potentially limits the accuracy and precision of δ^2H and $\delta^{18}O$. Therefore, we determined these analytical blanks using the STDs at least once a day (Gelwicks and Hayes, 1990; Tsunogai et al., 2000). The average analytical blank concentration and isotopic compositions of the system during the 11 months were 255 ± 149 ppmv (1σ) for H_2O concentration, −94 ± 31‰ (1σ) for δ^2H, and +27 ± 88‰ (1σ) for $\delta^{18}O$. The contribution of blank H_2O was subtracted from the measured concentration and isotopic compositions of the water vapor using Eq. (1) and based on the blank H_2O values determined on the same day.

To check that the blank correction was successful or not, we prepared samples J-2, K-2, and L-2 by diluting air samples J-1, K-1, and L-1 with dry air (Table 1). After correcting for the contribution of the analytical blank determined on the same day, the isotopic compositions of the diluted samples J-2, K-2, and L-2 coincided well (within 2σ analytical precision) with each original air sample (J-1, K-1, and L-1, respectively), while the contribution of blank H_2O in the diluted samples was 2–3 times larger than that in the original air samples. Additionally, the calculated H_2O concentrations of J-2, K-2, and L-2 were consistent with the original H_2O concentrations. Therefore, we concluded that any bias from blank H_2O had been successfully reduced through the in-situ collection method.

3.2. Cross-contamination

During successive measurements of H_2O isotopic compositions with a CRDS system, significant cross-contamination of residual H_2O injected and measured prior to each sample (memory effect) had been reported in previous studies (Gupta et al., 2009; Uemura et al., 2016). Assuming that only H_2O injected and measured just prior to each sample measurement influences, the apparent isotopic composition of the current i-th injection ($\delta_a(i)$) can be expressed using the formula (Uemura et al., 2016):

$$\delta_a(i) = X_i * \delta_P + (1-X_i) * \delta_C \tag{2}$$

where X_i is the memory coefficient of a previous sample on the i-th injection of the current sample, δ_P is the isotopic composition of the immediately previous sample, and δ_C is the isotopic composition of current sample. Uemura et al. (2016) also reported that the memory coefficient (X_i) depended on the amount of water introduced into the cavity during measurement of the current sample.

To quantify the X_i of the analytical system, successive analyses of air samples with water vapor consisting of various isotopic compositions were performed. The total quantity of H_2O (water vapor) injected into the cavity was estimated from the changes in glass bottle internal pressure during each analysis, as well as the internal volume of the glass bottles and the H_2O concentration in it. Each air sample was measured repeatedly (3 to 5 times), and isotopic compositions obtained during the last measurement of the repeat sample measurements were used as the isotopic compositions of previous and current samples (δ_P and δ_C, respectively). The difference in isotopic compositions between previous and current samples ranged from 12 to 72‰ for δ^2H, and 0.9 to 13.5‰ for $\delta^{18}O$, and the H_2O concentration of the air samples ranged from 1800 to 13,500 ppmv. The memory coefficients (X_i) were estimated by applying Eq. (2) to the last injection of the previous air sample and the first injection of the current sample (X_1), as well as to the last injection of the previous air sample and the second injection of the current sample (X_2) (Fig. 3). X_i decreased exponentially with increased H_2O injected into the analytical system, which is consistent with the previous study (Uemura et al., 2016).

The X_1 during the first injection was around 0.80 under an introduced water vapor quantity of 10 μmol for δ^2H (Fig. 3a). The X_1 of δ^2H can be described as a function of the water vapor quantities introduced (M) empirically: $X_1 = 5.741 * M^{-0.898}$ ($R^2 = 0.82$) for the first injections (11–141 μmol), and $X_2 = 269.82 * M^{-3.371}$ ($R^2 = 0.59$) for the second injections (7–98 μmol). As shown in Fig. 3a, the X_i for the second injections were almost zero when >30 μmol of water vapor were introduced. For the third injections, small values were observed for X_i. The maximum difference between δ^2H_a (3) and δ^2H_c was 9.5‰ when the quantities of water vapor injected were <7 μmol (which corresponds to about 2200 ppmv or less), and the δ^2H difference between δ^2H_P and δ^2H_C ($|\delta^2H_P - \delta^2H_C|$) was >60‰. The isotopic compositions of the fourth injections (δ^2H_a (4)) coincided with δ^2H_C within 2σ of the analytical precision, regardless of the water vapor quantity injected. Similar trends of X_i as a function of M were also observed for $\delta^{18}O$ (Fig. 3b), showing empirical curves of $X_1 = 10.304 * M^{-1.319}$ ($R^2 = 0.82$), and $X_2 = 39.075 * M^{-2.883}$ ($R^2 = 0.51$) for the first and second injections, respectively. The values of X_i of $\delta^{18}O$ for the second injections (X_2) were also

Table 1

The H_2O concentration, maxima, minima, and average isotopic compositions after blank correction determined repeatedly for each air sample in 1 L glass bottles with their standard deviations. The samples J-2, K-2, and L-2 were obtained by diluting J-1, K-1, and L-1 with dry air.

Sample name	n[a]	[H_2O][b] (ppmv)	1000 δ^2H (vs. VSMOW)				1000 $\delta^{18}O$ (vs. VSMOW)			
			Max.	Min.	Avg.	SD[c]	Max.	Min.	Avg.	SD
A	7	27,638	−166.1	−169.9	−168.8	1.4	−24.42	−24.71	−24.52	0.11
B	7	26,674	−167.6	−171.0	−169.8	1.3	−24.34	−24.74	−24.57	0.15
C	7	18,927	−155.4	−156.5	−155.9	0.4	−22.61	−23.63	−22.95	0.41
D	7	16,291	−157.1	−157.5	−157.2	0.1	−21.32	−22.47	−21.73	0.44
E	5	14,676	−165.1	−168.2	−166.9	1.4	−24.76	−25.49	−25.20	0.27
F	7	11,101	−169.5	−178.7	−175.0	3.2	−25.19	−25.88	−25.54	0.22
G	5	5707	−107.7	−110.7	−109.1	1.3	−19.84	−20.36	−20.12	0.23
H	7	5166	−104.3	−105.8	−105.1	0.6	−20.07	−20.72	−20.50	0.23
I	2	3386	−127.8	−128.2	−128.0	0.3	−23.05	−23.15	−23.10	0.07
J-1	2	5946	−119.2	−119.6	−119.4	0.3	−18.92	−19.10	−19.01	0.13
J-2	3	1818	−110.0	−118.3	−113.5	4.3	−19.13	−19.71	−19.52	0.33
K-1	1	4320	n.d.	n.d.	−121.1	n.d.	n.d.	n.d.	−20.97	n.d.
K-2	3	1798	−118.1	−119.2	−118.8	0.6	−21.33	−21.49	−21.38	0.10
L-1	2	5928	−120.6	−122.7	−121.7	1.4	−18.49	−18.51	−18.50	0.01
L-2	4	1811	−110.7	−119.2	−115.2	3.5	−18.76	−19.88	−19.42	0.47

n.d.: not determined.

[a] Number of repeated measurements except for the first twice injections to flush the analytical system.

[b] Corrected concentration of H_2O using the Eq. (5) (see Section 3.4. for the details).
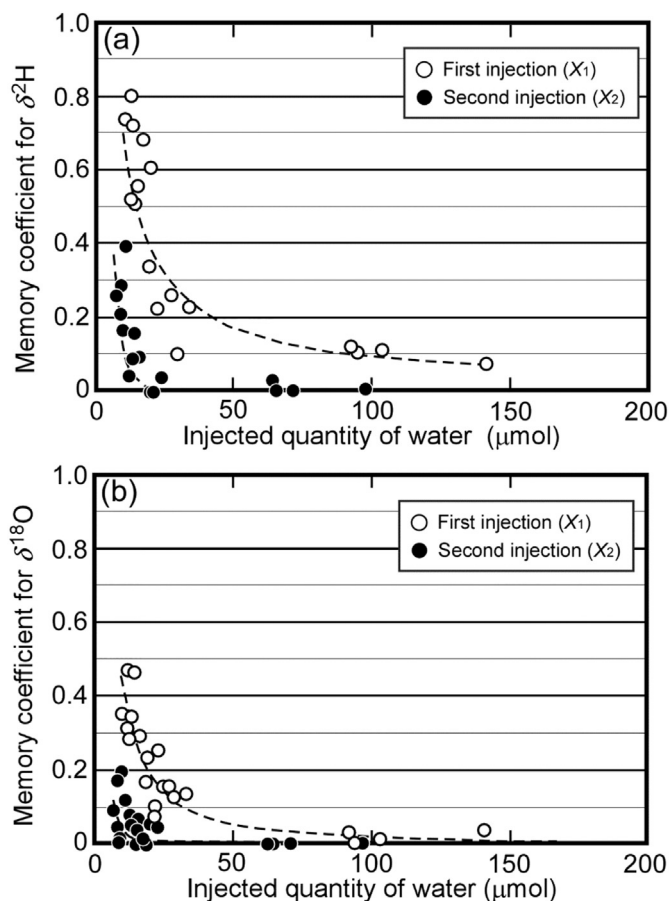
[c] Standard deviations.

Fig. 3. Memory coefficients for δ^2H (a) and $\delta^{18}O$ (b) plotted as a function of the amount of water vapor injected into the analytical system. The circles are memory coefficients, X_i, for the first (open circle) and second (filled circle) injections. The dashed lines represent the best fit curves for the X_i values of the first and second injections.

negligible when >30 μmol of injected H_2O were introduced. The measured $\delta^{18}O$ of the third injections ($\delta^{18}O_a$ (3)) coincided with $\delta^{18}O_c$ within 2σ, regardless of the quantities of water vapor injected. The values of X_i of $\delta^{18}O$ were less than δ^2H. Similar results were also obtained during measurements using the CRDS system (Gupta et al., 2009; Uemura et al., 2016).

We routinely measured air/volcanic plume samples in each glass bottle through successive, repeated injections more than 3 times and estimated isotopic compositions from the third injection or later, if we had sufficient quantities of volcanic plume/air samples. As a result of these experiments, we chose a sample volume 1 L of the volcanic plume.

3.3. Analytical precision

To check the analytical precision of δ^2H and $\delta^{18}O$ values using our system, air samples with various H_2O concentrations were prepared in 1 L glass bottles and measured repeatedly using the system. The average δ^2H and $\delta^{18}O$ values and their standard deviations (1σ) are listed in Table 1, together with H_2O concentrations. The analytical precision (1σ) of δ^2H and $\delta^{18}O$ during a single analysis was estimated to be better than 2‰ and 0.3‰, respectively, when >3400 ppmv of H_2O in a 1 L glass bottle was introduced, and better than 3‰ (δ^2H) and 0.4‰ ($\delta^{18}O$) when >1800 ppmv of H_2O was introduced (Table 1). Changes in the H_2O isotopic compositions in accordance with concentration had been found in previous studies using CRDS (Brand et al., 2009; Arienzo et al., 2013) and was likely a result in changes in the contribution of the blank H_2O. While blank H_2O contributions were removed from the isotopic compositions listed in Table 1, the precision was worse when H_2O

concentrations were low because of fluctuations in the blank H_2O isotopic compositions.

Changes in the isotopic compositions as a function of sample bottle internal pressure were tested and are shown in Fig. 4. There was no systematic variation in the determined isotopic compositions with internal pressure between 1.0 and 0.2 atm. However, apparent H_2O concentrations tended to decrease systematically from the initial measurements at 1.0 atm with internal pressure in the glass bottle (Fig. 4). The relative changes in the apparent H_2O concentration can be described using an empirical equation:

$$R_{H2O} \, (\%) = -0.4393 * P^{-1.9544} + 100.34 \, \left(R^2 > 0.99 \right) \tag{3}$$

where R_{H2O} denotes the apparent concentration relative to the original (in %) determined under 1 atm, and P (in atm) denotes the internal pressure in a 1 L glass bottle. Moreover, change in the internal pressure after a single isotopic analysis using our system can be also described as a function of the internal pressure at the start of injection using an empirical equation:

$$R_P \, (\%) = 72.369 * P^{-0.056} \, \left(R^2 = 0.98 \right) \tag{4}$$

where R_P denotes the change in the internal pressure relative to the initial pressure (in %). Changes in the internal pressure during repeated measurements of the same sample, therefore, can be calculated from Eq. (4) and the internal pressure before the repeated measurements. Then, R_{H2O} was calculated from internal pressure (P) at the start of injection and used to correct the apparent H_2O concentration obtained during each analysis under 1 atm.

3.4. Comparison with the cold trap method

To check the analytical accuracy of atmospheric/volcanic H_2O concentrations and isotopic compositions determined through our in-situ collection method and the analytical system, we analyzed the H_2O concentration and isotopic compositions in laboratory air with our in-situ collection method and, simultaneously, the traditional cold trap method. In the cold trap method, laboratory air with water vapor was introduced into two cold traps made from U-shaped glass tubes (10 mm i.d.) and held at a dry ice + ethanol temperature of −70 °C. The end of the first U-shaped glass tube was filled with 2 cm glass wool; the second tube was kept empty. The flow rate was set at 2 L/min using an air pump with a mass flow controller and integrating flowmeter (GSP-2LFT, Gastec Corp., Japan). At the end of the sampling period, the air pump was stopped, and the dry ice + ethanol was removed, and both ends of the cold traps were sealed immediately with parafilm. The average H_2O concentration in the laboratory air during each sampling period was calculated from the water condensate weight, determined from the change in weight of the two cold traps before and after the collection and the total air volume (100 or 150 L) measured by the integrating flowmeter. There was no apparent water condensate (or ice) in the second U-shaped glass tube. The collected water vapor (ice) samples were melted and transferred into glass vials (2 mL glass short-thread vial, PTFE/silicone capped) for the CRDS isotopic composition measurements by introducing the liquid H_2O into the vaporizer (Gupta et al., 2009; Nakagawa et al., 2018; Tsunogai et al., 2018). Simultaneous to the cold trap sampling, several laboratory air samples (n = 3 or 6) including the beginning and end of the sampling were also taken into pre-evacuated 1 L glass bottles for measurement of the average H_2O concentration and isotopic compositions in laboratory air using our in-situ collection method.

The in-situ collection method tended to show slightly higher isotopic compositions compared to the cold trap method irrespective to the values determined, +3.4 ± 2.4‰ (averaged ±1σ) for δ^2H and +1.02 ± 0.49‰ for $\delta^{18}O$ (Table 2), respectively. An insufficient collection of

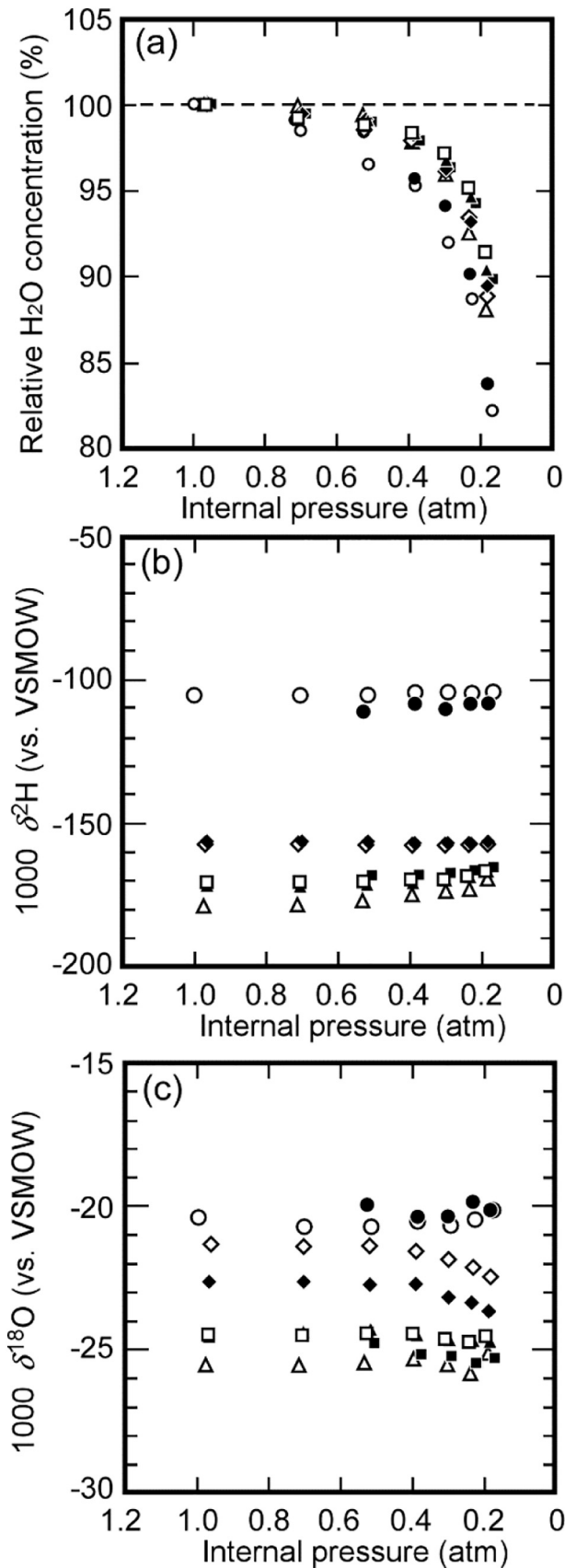**Fig. 4.** Apparent variation in concentration (a) and the δ^2H (b) and $\delta^{18}O$ (c) of atmospheric water vapor in 1-L glass bottle during repeated measurements of the same sample plotted as a function of the internal pressure of each bottle. The same legend (e.g., triangle, square, circle) denotes the same sample bottle.

atmospheric water vapor during the cold trap method and thus isotopic fractionation during the collection cannot be responsible for the discrepancies because the isotopic compositions of water condensate should be higher than the total water vapor due to preferential condensation of H_2O with heavier isotopes. Rather, isotopic fractionation processes during sampling and/or sample injection could be responsible for the discrepancies. In this study, after introducing the sample into cavity cell, the isotopic compositions of liquid sample were calculated by averaging the data collected for about 120 s (Gupta et al., 2009), while those of vapor sample (bottle sample) were calculated by averaging the data collected for 270 s. Our preliminary experiments for the determining measurement time showed that the measured $\delta^{18}O$ and δ^2H values tended to increase slightly with increasing the measurement time. The different isotopic fractionation effects originating in the measurement time could be responsible for the discrepancies. In any case, the differences were small compared with the variation in the isotopic compositions of atmospheric water vapor. As a result, we corrected for the deviations from each measured data point obtained by the in-situ collection method throughout this study, assuming that the values determined through the cold trap method were reliable.

The H_2O concentrations determined by the in-situ collection method also showed small deviations from those determined by the cold trap method throughout the analyses (Table 2) and exhibited a slope <1 (Fig. 5). We therefore normalized to the raw H_2O concentrations from the in-situ collection method by the cold trap method using a linear regression equation:

$$[H_2O]_{corrected} = 0.8637 * [H_2O]_{raw} \qquad (5)$$

where $[H_2O]_{corrected}$ is the H_2O concentration corrected to the cold trap method, and $[H_2O]_{raw}$ is the raw H_2O concentration under at 1 atm obtained through the in-situ collection method after correction for the contribution of blank H_2O. Because the uncertainty in the volume determined by the air pump was 5%, we estimated the error in the H_2O concentration to be ±5%.

3.5. Influence of SO_2 and H_2S

Volcanic plumes in general contain SO_2, with SO_2/H_2O ratios up to 0.01 (Aiuppa et al., 2005; Shinohara, 2005, 2013; Shinohara et al., 2008). As a result of this, we performed additional experiments to assess the influence of SO_2 in our analytical system. The isotopic compositions of atmospheric H_2O sampled in glass bottles were compared with the same atmospheric sample after mixing with a gas that contained 522 ppm SO_2 in a dry air matrix (Japan Fine Products Corp., Japan). The SO_2 concentration of the mixed air samples ranged from 0 to 31 ppm.

The differences in isotopic compositions from the original air samples ($\Delta\delta^2H$ and $\Delta\delta^{18}O$) were plotted as a function of the SO_2/H_2O ratio (Fig. 6). The average deviations from the original air samples were $-0.1 \pm 1.4‰$ (1σ) for $\Delta\delta^2H$ and $+0.33 \pm 0.15‰$ (1σ) for $\Delta\delta^{18}O$. The average deviations are smaller than the analytical precision. Moreover, we did not find significant changes in $\Delta\delta^2H$ and $\Delta\delta^{18}O$ in accordance with an increase in the SO_2/H_2O ratio. We thus concluded that the influence of SO_2 on the isotopic compositions of H_2O were almost negligible when the SO_2/H_2O ratios was <0.003 (Fig. 6).

The changes in the isotopic compositions from the original air sample were also plotted as a function of H_2S/H_2O ratio (Fig. 6). The average deviations between the original air samples and H_2S/air mixtures were $-0.3 \pm 2.1‰$ (1σ) for $\Delta\delta^2H$ and $+0.11 \pm 0.28‰$ (1σ) for $\Delta\delta^{18}O$. For CO_2 isotopic measurements using CRDS techniques, the differences between the measured and true CO_2 isotopic compositions depend on the H_2S/CO_2 ratios (Malowany et al., 2015). Although the influence of H_2S on the isotopic compositions of H_2O might be observed under high H_2S/H_2O ratios, we did not find significant changes in $\Delta\delta^2H$ and $\Delta\delta^{18}O$ in accordance with an increase under H_2S/H_2O ratios <0.003. We concluded

Table 2

Comparison of H_2O concentration and isotopic compositions (δ^2H and $\delta^{18}O$) of atmospheric water vapor in laboratory air using our in-situ collection method (δ_{bottle}) and the cold trap method (δ_{trap}).

Run code	ppmv		1000 δ^2H (vs. VSMOW)			1000 $\delta^{18}O$ (vs. VSMOW)		
	Bottle	Cold trap	δ_{bottle}	δ_{trap}	$\delta_{bottle}-\delta_{trap}$	δ_{bottle}	δ_{trap}	$\delta_{bottle}-\delta_{trap}$
1	7252	6034	−104.2	−106.3	+2.1	−17.93	−18.18	+0.25
2	8447	6811	−98.3	−104.3	+6.0	−16.45	−17.50	+1.05
3	8592	6518	−99.0	−105.0	+6.0	−16.31	−17.92	+1.61
4	14,577	13,167	−81.9	−82.6	+0.8	−11.54	−12.67	+1.13
5	19,084	16,748	−77.2	−79.4	+2.3	−11.51	−12.59	+1.08
Avg. ± SD[a]					+3.4 ± 2.4			+1.02 ± 0.49

[a] Standard deviations.

that the influence of H_2S on the H_2O isotopic compositions was also negligible under H_2S/H_2O ratios <0.003 (Fig. 6).

3.6. Field Samples

Our in-situ collection method and the analytical system allow determination of variable H_2O concentrations and isotopic compositions in volcanic plume samples. To further validate the method and demonstrate its applicability, a field study was carried out in a fumarolic area.

The Kirishima volcano group (the Kirishima group), located at the northernmost end of the southern Kyushu volcanic chain, and is one of the most active volcano groups in Japan. They consist of more than 20 Quaternary volcanic cones within an area of ~20 × 30 km. Two calderas (Kakuto and Kobayashi) are located in the northern sector of the Kirishima Volcanoes, where some 100 km³ of magma was extruded between ~300 and ~500 ka (Tajima and Aramaki, 1980; Imura, 1994).

Iwo-yama is one of the active volcanoes in the Kirishima group and has an active fumarolic area on its southern flank. The volcanic plume samples were taken from one Iwo-yama fumarole on 25 July 2017. Immediately prior to volcanic plume sampling, a water condensate sample for δ^2H and $\delta^{18}O$ analyses was collected directly at the fumarole (148 °C) using a glass condenser cooled to 0 °C. Then, the volcanic plume samples were taken into pre-evacuated 1 L glass bottles that had two stopcocks sealed by Viton o-rings until ambient atmospheric pressure was reached. The samples were taken along the axis of the plume by moving outward from the targeted fumarole. We also took samples of background air at a point distant and, if possible, upwind from the fumarolic area. These background air samples were taken at the beginning and end of the volcanic plume sampling. The H_2O concentration and isotopic compositions of background air samples ranged from 27,520 to 28,078

ppmv, −19.11 to −18.90‰ for $\delta^{18}O$, and −122.2 to −123.0‰, suggesting that the fluctuation in background air during the volcanic plume sampling was very small.

Ohba et al. (2017) reported that the SO_2/H_2O and H_2S/H_2O ratios in the fumarolic gases were <0.003, during 2017. The H_2O concentrations of the plume samples ranged from 29,700 to 42,000 ppmv. As a result, we concluded that the influence of SO_2 and H_2S on the H_2O isotopic compositions from the volcanic plume was negligible. As shown in Fig. 7, the reciprocal of the H_2O concentration (1/[H_2O] (‰$^{-1}$)) in the
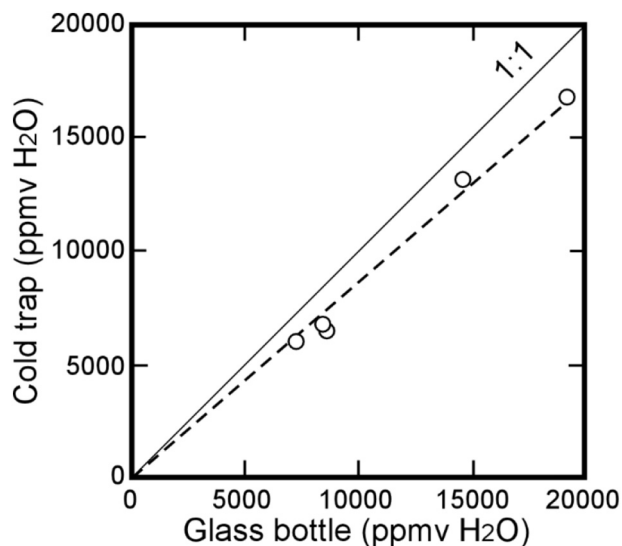

Fig. 5. Comparison of the average H_2O concentration in laboratory air determined by the cold trap method and the in-situ collection method (Glass bottle) (R^2 > 0.98).
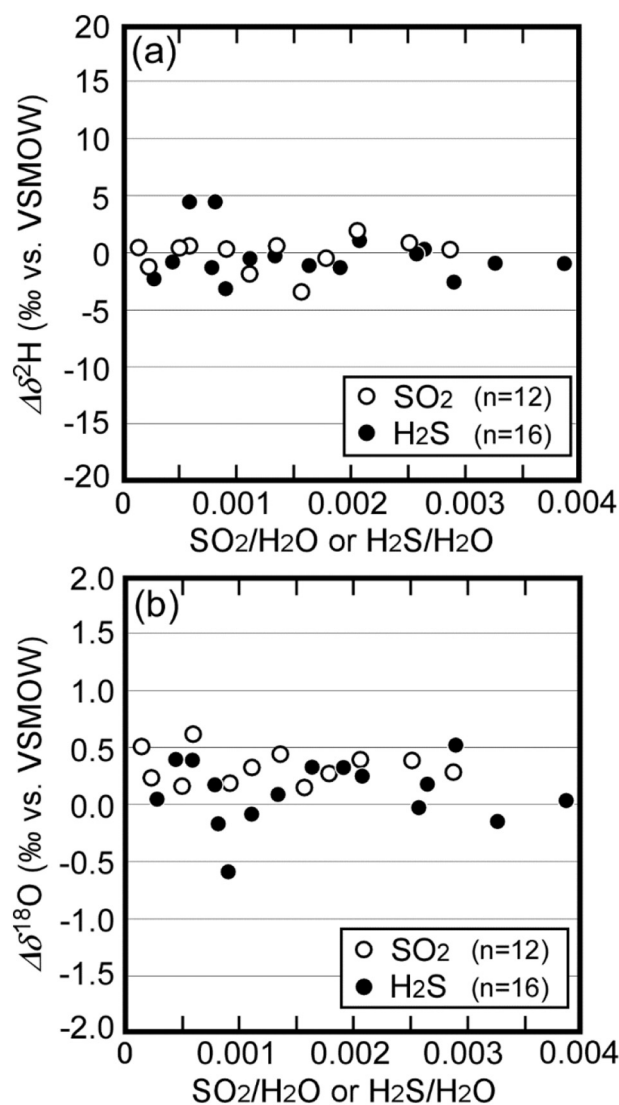

Fig. 6. Changes in the apparent isotopic compositions of δ^2H (a) and $\delta^{18}O$ (b) from the original air sample as a result of SO_2 (or H_2S) addition to each sample plotted as a function of the SO_2/H_2O and H_2S/H_2O ratios.
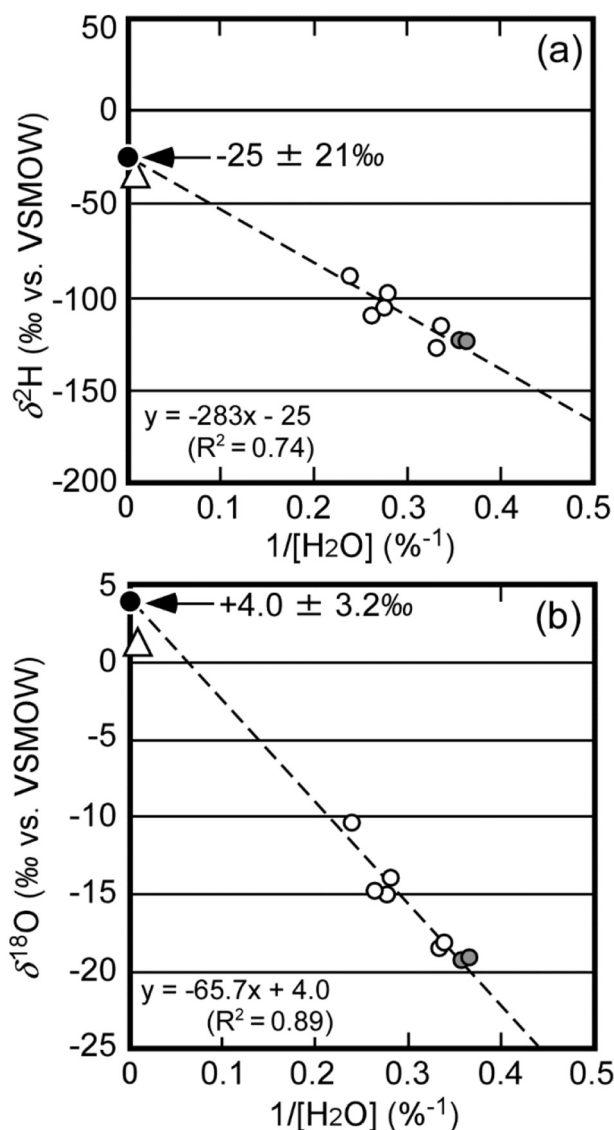
Fig. 7. Relationship between the δ^2H (a) and $\delta^{18}O$ (b) of H_2O and the reciprocal of H_2O concentration in the Iwo-yama volcanic plume, together with the estimated isotopic compositions (δ^2H and $\delta^{18}O$) of fumarolic H_2O by keeling approach (closed circles). The grey circles are background air samples. The dotted line is the least squares fitting to the plume/background air samples. The open triangles at $1/[H_2O] = 0.01$ ($\%^{-1}$) are the isotopic compositions of actual fumarolic H_2O (water condensate).

plume samples showed a good linear relationship with the isotopic compositions. The linear relationships suggested that the concentration and isotopic composition in samples from each site can be explained by simple mixing between two end-members, each of which can be classified into a single category (Keeling, 1958; Tsunogai et al., 1998,2005, 2010,2011). By extrapolating the linear relationships between $1/[H_2O]$ ($\%^{-1}$) and stable isotopic compositions to $1/[H_2O] = 0$ ($\%^{-1}$) to exclude the contribution of H_2O in background air (H_2O-depleted end-member) from the sample isotopic compositions (Keeling, 1958; York, 1966; Tsunogai et al., 2003,2010), we estimated the δ^2H ($-25 \pm 21\permil$, 68% confidence interval) and $\delta^{18}O$ ($+4.0 \pm 3.2\permil$, 68% confidence interval) values of fumarolic H_2O (H_2O-enriched end-member) (Fig. 7) through least squares fitting of the straight lines. Because the data errors were variable, particularly in $1/[H_2O]$ ($\%^{-1}$), we fitted each line taking into account the differences in the errors (York, 1966).

The $1/[H_2O]$ ($\%^{-1}$) values of fumarolic H_2O should be larger than 0, irrespective of the actual $[H_2O]$ in fumarolic gas. As a result, the isotopic compositions of the H_2O-enriched end-members must be lower than the estimated isotopic compositions. The H_2O concentration of the

fumarolic gas in Iwo-yama is generally >98% (Ohba et al., 2017), corresponding to a $1/[H_2O]$ value of almost 0.01 ($\%^{-1}$). Because the slope of the linear fitted relationship between $1/[H_2O]$ and δ^2H (Fig. 7) was 283‰ per $\%^{-1}$, the difference between calculated ($1/[H_2O] = 0$) and actual ($1/[H_2O] = 0.01$) should be <3‰. In the same manner, the difference should be <0.7‰ for the estimation of $\delta^{18}O$. These differences were much smaller than the fitting error (Fig. 7). As a result, we disregarded these differences and used 0 for the $1/[H_2O]$ values of the H_2O-enriched end-members.

The isotopic differences between the keeling intercept and water condensate could be caused by heterogeneities in the isotopic compositions of fumarolic H_2O in the fumarolic area, since volcanic plume can be derived not only from one (targeted) fumarole, but from many other fumaroles located in the fumarolic area. Although there were some differences between the keeling intercept and water condensate, the isotopic compositions of fumarolic H_2O from the Iwo-yama volcanic plume corresponded to the water condensate ($\delta^2H = -36\permil$ and $\delta^{18}O = +1.0\permil$) within the fitting error. As a result, we concluded that we can deduce the isotopic compositions of fumarolic H_2O without sampling fumarolic gases directly, by determining the H_2O concentration and isotopic composition of its volcanic plume and then correcting for the contribution of background H_2O. Although more studies are required to verify our results, they suggest that we can estimate the isotopic compositions of fumarolic H_2O remotely using the sampling and analytical system presented in this study.

4. Conclusions

A simple, rapid, and convenient CRDS analytical system was developed to determine atmospheric/volcanic water vapor concentration and isotopic compositions (δ^2H and $\delta^{18}O$). Analytical precision (standard deviation of a single analysis) was estimated to be better than 2‰ and 0.3‰, respectively, when >3400 ppmv of H_2O was introduced, and better than 3‰ (δ^2H) and 0.4‰ ($\delta^{18}O$) when >1800 ppmv of H_2O was introduced. Using our new analytical system, we deduced the isotopic compositions of fumarolic H_2O from Iwo-yama volcanic plume samples (the Kirishima group). The estimated isotopic compositions were consistent with actual fumarolic H_2O (water condensate) isotopic compositions within the fitting error. As a result, the new analytical system enables us to remotely assess the type of volcanic eruption, without sampling fumarolic gases directly. In comparison with traditional cold trap methods, the new system also has advantages in that we can determine fumarolic H_2O isotopic compositions without tedious, time consuming, and dangerous sampling in fumarolic areas of active volcanoes.

References

Aiuppa, A., Federico, C., Giudice, G., Gurrieri, S., 2005. Chemical mapping of a fumarolic field: La Fossa Crater, Vulcano Island (Aeolian Islands, Italy). Geophys. Res. Lett. 13, L13309. https://doi.org/10.1029/2005GL023207.

Aiuppa, A., Bertagnini, A., Métrich, N., Moretti, R., Di Muro, A., Liuzzo, M., Tamburello, G., 2010. A model of degassing for Stromboli volcano. Earth Planet. Sci. Lett. 295, 195–204.

Aiuppa, A., Shinohara, H., Tamburello, G., Giudice, G., Liuzzo, M., Moretti, R., 2011. Hydrogen in the gas plume of an open-vent volcano, Mount Etna, Italy. J. Geophys. Res. Solid Earth 116, B10204. https://doi.org/10.1029/2011JB008461.

Arienzo, M.M., Swart, P.K., Vonhof, H.B., 2013. Measurement of $\delta^{18}O$ and δ^2H values of fluid inclusion water in speleothems using cavity ring-down spectroscopy compared with isotope ratio mass spectrometry. Rapid Commun. Mass Spectrom. 27, 2616–2624. https://doi.org/10.1002/rcm.6723.

Barberi, F., Bertagnini, A., Landi, P., Principe, C., 1992. A review on phreatic eruptions and their precursors. J. Volcanol. Geotherm. Res. 52, 231–246.

Bastrikov, V., Steen-Larsen, H.C., Masson-Delmotte, V., Gribanov, K., Cattani, O., Jouzel, J., Zakharov, V., 2014. Continuous measurements of atmospheric water vapour isotopes in western Siberia (Kourovka). Atmos. Meas. Tech. 7, 1763–1776.

Brand, W.A., Geilmann, H., Crosson, E.R., Rella, C.W., 2009. Cavity ring-down spectroscopy versus high-temperature conversion isotope ratio mass spectrometry: a case study on δ^2H and $\delta^{18}O$ of pure water samples and alcohol/water mixtures. Rapid Commun. Mass Spectom. 23, 1879–1884. https://doi.org/10.1002/rcm.4083.

Coplen, T.B., Hopple, J., 1995. Audit of VSMOW distributed by the United States National Institute of Standards and Technology. Reference and Intercomparison Materials for Stable Isotopes of Light Elements. *Proceedings of a Consultants Meeting Held in Vienna, 1–3 December 1993.* IAEA, pp. 51–66.

Craig, H., 1961. Isotopic variations in meteoric waters. Science 133, 1702–1703.

Craig, H., 1963. The isotopic geochemistry of water and carbon in geothermal areas. In: Tongiorgi, E. (Ed.), Proceedings of the Spoleto Conference on Nuclear Geology on Geothermal Areas, pp. 17–53 Pisa, Italy.

Craig, H., Gordon, L.I., 1965. Deuterium and oxygen 18 variations in the ocean and the marine atmosphere. In: Tongiorgi, E. (Ed.), Proceedings of Stable Isotopes in Oceanographic Studies and Paleotemperatures, pp. 9–130 Spoleto, Italy.

Fischer, T.P., Lopez, T.M., 2016. First airborne samples of a volcanic plume for $\delta^{13}C$ of CO_2 determinations. Geophys. Res. Lett. 43, 3272–3279. https://doi.org/10.1002/2016GL068499.

Gelwicks, J.T., Hayes, J.M., 1990. Carbon-isotopic analysis of dissolved acetate. Anal. Chem. 62, 535–539.

Giggenbach, W.F., 1987. Redox processes governing the chemistry of fumarolic gas discharges from White Island, New Zealand. Appl. Geochem. 2, 143–161.

Giggenbach, W.F., 1992. Isotopic shifts in waters from geothermal and volcanic systems along convergent plate boundaries and their origin. Earth Planet. Sci. Lett. 113, 495–510.

Giggenbach, W.F., Matsuo, S., 1991. Evaluation of results from Second and Third IAVCEI Field Workshops on volcanic gases, Mt. Usu, Japan and White Island, New Zealand. Appl. Geochem. 6, 125–141.

Griffith, D.W.T., Jamie, I., Esler, M., Wilson, S.R., Parkes, S.D., Waring, C., Bryant, G.W., 2006. Real-time field measurements of stable isotopes in water and CO_2 by Fourier transform infrared spectrometry. Isot. Environ. Health Stud. 42, 9–20. https://doi.org/10.1080/10256010500503098.

Gupta, P., Noone, D., Galewsky, J., Sweeney, C., Vaughn, B.H., 2009. Demonstration of high-precision continuous measurements of water vapor isotopologues in laboratory and remote field deployments using wavelength-scanned cavity ring-down spectroscopy (WS-CRDS) technology. Rapid Commun. Mass Spectrom. 23, 2534–2542. https://doi.org/10.1002/rcm.4100.

Iannone, R.Q., Romanini, D., Cattani, O., Meijer, H.A.J., Kerstel, E.R.T., 2010. Water isotope ratio (δ^2H and $\delta^{18}O$) measurements in atmospheric moisture using an optical feedback cavity enhanced absorption laser spectrometer. J. Geophys. Res. Atmos. 115, D10111. https://doi.org/10.1029/2009JD012895.

Imura, R., 1994. Geology of Kirishima volcano. Bull. Earthquake. Res. Inst. Univ. Tokyo 69, 189–209 (in Japanese with English abstract).

Keeling, C.D., 1958. The concentration and isotopic abundances of atmospheric carbon dioxide in rural areas. Geochim. Cosmochim. Acta 13, 322–334.

Kerstel, E.R.T., 2004. Isotope ratio infrared spectrometry. In: de Groot, P.A. (Ed.), Handbook of Stable Isotope Analytical Techniques. vol. volume I. Elsevier, Amsterdam, pp. 759–787.

Lee, X., Sargent, S., Smith, R., Tanner, B., 2005. In situ measurement of the water vapor $^{18}O/^{16}O$ isotope ratio for atmospheric and ecological applications. J. Atmos. Ocean. Technol. 22, 555–565.

Malowany, K., Stix, J., Van Pelt, A., Lucic, G., 2015. H_2S interference on CO_2 isotopic measurements using a Picarro G1101-i cavity ring-down spectrometer. Atmos. Meas. Tech. 8, 4075–4082. https://doi.org/10.5194/amt-8-4075-2015.

Malowany, K.S., Stix, J., de Moor, J.M., Chu, K., Lacrampe-Couloume, G., Sherwood Lollar, B., 2017. Carbon isotope systematics of Turrialba volcano, Costa Rica, using a portable cavity ring-down spectrometer. Geochem. Geophys. Geosyst. 18, 2769–2784. https://doi.org/10.1002/2017GC006856.

Matsuo, S., Suzuoki, T., Kusakabe, M., Wada, H., Suzuki, M., 1974. Isotopic and chemical compositions of volcanic gases from Satsuma-Iwojima, Japan. Geochem. J. 8, 165–173.

Matsuo, S., Kusakabe, M., Niwano, M., Hirano, T., Oki, Y., 1985. Origin of thermal waters from the Hakone geothermal system, Japan. Geochem. J. 19, 27–44.

Nakagawa, F., Tsunogai, U., Obata, Y., Ando, K., Yamashita, N., Saito, T., Uchiyama, S., Morohashi, M., Sase, H., 2018. Export flux of unprocessed atmospheric nitrate from temperate forested catchments: a possible new index for nitrogen saturation. Biogeosciences 15, 7025–7042.

Ohba, T., Daita, Y., Sawa, T., Taira, N., Kakuage, Y., 2011. Coseismic changes in the chemical composition of volcanic gases from the Owakudani geothermal area on Hakone Volcano, Japan. Bull. Volcanol. 73, 457–469.

Ohba, T., Nishino, K., Numanami, N., Taniguchi, M., Takagi, A., Shinohara, H., Kazahaya, R., 2017. Chemical composition and stable isotope ratio of the fumarolic gases sampled at Iwo-yama volcano, Kirishima, Japan (Dec. 2015 to May 2017). Report of the Coodinating Committee for Prediction of Volcanic Eruptions 127, 318–327 (in Japanese).

Picarro, Inc, 2012. Data Sheet PICARRO L2120-i $\delta D/\delta^{18}O$ Isotopic Water Analyzer (Santa Clara, CA, USA, 2 pgs).

Rizzo, A.L., Jost, H.J., Caracausi, A., Paonita, A., Liotta, M., Martelli, M., 2014. Real-time measurements of the concentration and isotope composition of atmospheric and volcanic CO_2 at Mount Etna (Italy). Geophys. Res. Lett. 41, 2382–2389. https://doi.org/10.1002/2014GL059722.

Rizzo, A.L., Liuzzo, M., Ancellin, M.A., Jost, H.J., 2015. Real-time measurements of $\delta^{13}C$, CO_2 concentration, and CO_2/SO_2 in volcanic plume gases at Mount Etna, Italy, over 5 consecutive days. Chem. Geol. 411, 182–191.

Schauer, A.J., Schoenemann, S.W., Steig, E.J., 2016. Routine high-precision analysis of triple water-isotope ratios using cavity ring-down spectroscopy. Rapid Commun. Mass Spectrom. 30, 2059–2069.

Schneider, M., Hase, F., 2009. Ground-based FTIR water vapour profile analyses. Atmos. Meas. Tech. 2, 609–619.

Shinohara, H., 2005. A new technique to estimate volcanic gas composition: plume measurements with a portable multi-sensor system. J. Volcanol. Geotherm. Res. 143, 319–333.

Shinohara, H., 2013. Composition of volcanic gases emitted during repeating Vulcanian eruption stage of Shinmoedake, Kirishima volcano, Japan. Earth Planets Space 65, 667–675.

Shinohara, H., Aiuppa, A., Giudice, G., Gurrieri, S., Liuzzo, M., 2008. Variation of H_2O/CO_2 and CO_2/SO_2 ratios of volcanic gases discharged by continuous degassing of Mount Etna, volcano, Italy. J. Geophys. Res. Solid Earth 113, B09203. https://doi.org/10.1029/2007JB005185.

Tajima, H., Aramaki, S., 1980. Bouguer gravity anomaly around Kirishima volcanoes, Kyusyu. Bull. *Earthquake Res. Inst. Univ. Tokyo* 55, 241–257 (in Japanese with English abstract).

Tremoy, G., Vimeux, F., Cattani, O., Mayaki, S., Souley, I., Favreau, G., 2011. Measurements of water vapor isotope ratios with wavelength-scanned cavity ring-down spectroscopy technology: new insights and important caveats for deuterium excess measurements in tropical areas in comparison with isotope-ratio mass spectrometry. Rapid Commun. Mass Spectrom. 25, 3469–3480. https://doi.org/10.1002/rcm.5252.

Tsunogai, U., Ishibashi, J., Wakita, H., Gamo, T., 1998. Methane-rich plumes in the Suruga Trough (Japan) and their carbon isotopic characterization. Earth Planet. Sci. Lett. 160, 97–105.

Tsunogai, U., Nakagawa, F., Hachisu, Y., Yoshida, N., 2000. Stable carbon and oxygen isotopic analysis of carbon monoxide in natural waters. Rapid Commun. Mass Spectrom. 14, 1507–1512.

Tsunogai, U., Hachisu, Y., Komatsu, D.D., Nakagawa, F., Gamo, T., Akiyama, K., 2003. An updated estimation of the stable carbon and oxygen isotopic compositions of automobile CO emissions. Atmos. Environ. 37, 4901–4910.

Tsunogai, U., Nakagawa, F., Gamo, T., Ishibashi, J., 2005. Stable isotopic compositions of methane and carbon monoxide in the Suiyo hydrothermal plume, Izu-Bonin arc: tracers for microbial consumption/production. Earth Planet. Sci. Lett. 237, 326–340.

Tsunogai, U., Kosaka, A., Nakayama, N., Komatsu, D.D., Konno, U., Kameyama, S., Nakagawa, F., Sumino, H., Nagao, K., Machiyama, H., 2010. Origin and fate of deep-sea seeping methane bubbles at Kuroshima Knoll, Ryukyu forearc region, Japan. Geochem. J. 44, 461–476.

Tsunogai, U., Kamimura, K., Anzai, S., Nakagawa, F., Komatsu, D.D., 2011. Hydrogen isotopes in volcanic plumes: tracers for remote temperature sensing of fumaroles. Geochim. Cosmochim. Acta 75, 4531–4546.

Tsunogai, U., Cheng, L., Ito, M., Komatsu, D.D., Nakagawa, F., Shinohara, H., 2016. Remote determinations on fumarole outlet temperatures in an eruptive volcano. Geophys. Res. Lett. 43, 11620–11627. https://doi.org/10.1002/2016GL070838.

Tsunogai, U., Miyauchi, T., Ohyama, T., Komatsu, D.D., Ito, M., Nakagawa, F., 2018. Quantifying nitrate dynamics in a mesotrophic lake using triple oxygen isotopes as tracers. Limnol. Oceanogr. 63, S458–S476.

Uemura, R., Matsui, Y., Yoshimura, K., Motoyama, H., Yoshida, N., 2008. Evidence of deuterium excess in water vapor as an indicator of ocean surface conditions. J. Geophys. Res. Atmos. 113, D19114. https://doi.org/10.1029/2008JD010209.

Uemura, R., Nakamoto, M., Asami, R., Mishima, S., Gibo, M., Masaka, K., Jin-Ping, C., Wu, C.C., Chang, Y.W., Shen, C.C., 2016. Precise oxygen and hydrogen isotope determination in nanoliter quantities of speleothem inclusion water by cavity ring-down spectroscopic techniques. Geochim. Cosmochim. Acta 172, 159–176.

Ueta, A., Sugimoto, A., Iijima, Y., Yabuki, H., Maximov, T.C., Velivetskaya, T.A., Ignatiev, A.V., 2013. Factors controlling diurnal variation in the isotopic composition of atmospheric water vapour observed in the taiga, eastern Siberia. Hydrol. Process. 27, 2295–2305.

Ueta, A., Sugimoto, A., Iijima, Y., Yabuki, H., Trofim, C.M., 2014. Contribution of transpiration to the atmospheric moisture in eastern Siberia estimated with isotopic composition of water vapour. Ecohydrol. 7, 197–208. https://doi.org/10.1002/eco.1403.

Wen, X.F., Sun, X.M., Zhang, S.C., Yu, G.R., Sargent, S.D., Lee, X., 2008. Continuous measurement of water vapor D/H and $^{18}O/^{16}O$ isotope ratios in the atmosphere. J. Hydrol. 349, 489–500.

York, D., 1966. Least-squares fitting of a straight line. Can. J. Phys. 44, 1079–1086.

Yu, W., Tian, L., Ma, Y., Xu, B., Qu, D., 2015. Simultaneous monitoring of stable oxygen isotope composition in water vapour and precipitation over the central Tibetan Plateau. Atmos. Chem. Phys. 15, 10251–10262. https://doi.org/10.5194/acp-15-10251-2015.